

## ON THE HIGH-ENERGY EMISSION OF THE PULSAR PSR B1055–52

G. E. Romero<sup>1</sup>Instituto Astronômico e Geofísico, USP, Brazil, and  
Instituto Argentino de Radioastronomía, Argentina

Received 1997 July 16; accepted 1998 February 20

## RESUMEN

PSR B1055–52 es uno de los pocos pulsares que han sido detectados en todos los rangos de energía, desde radio hasta rayos  $\gamma$ . Es también el pulsar que posee la mayor eficiencia para convertir energía rotacional en emisión  $\gamma$ . En el presente trabajo se discuten los principales mecanismos que pueden generar la radiación de altas energías en este objeto y se comparan las diferentes predicciones con datos recientes obtenidos por los satélites *ROSAT*, *ASCA* y *Compton*. La estimación de la distancia al pulsar basada en la medida de dispersión es reconsiderada en vista de los resultados.

## ABSTRACT

PSR B1055–52 is one of the very few pulsars detected at all energy bands, from radio to  $\gamma$ -rays. It is also the pulsar with the highest efficiency for converting rotational energy in  $\gamma$ -ray emission. In this paper, the main mechanisms that could generate the high-energy emission in this object are discussed and different predictions from the main models are compared with recent data obtained by *ROSAT*, *ASCA*, and *Compton* satellites. The dispersion measure distance to the pulsar is reconsidered in the light of the results.

**Key words:** GAMMA RAYS–THEORY — STARS–NEUTRON —  
STARS–PULSARS–INDIVIDUAL (PSR B1055–52) —  
X-RAYS–STARS

## 1. INTRODUCTION

The pulsar PSR B1055–52 (=PSR J1057–5226) was discovered by Vaughan & Large (1972). It has a relatively short period of 197.11 m with a derivative of  $5.8 \times 10^{-15} \text{ s s}^{-1}$ . From these values a dynamic age of  $\tau = P/2\dot{P} \sim 5.3 \times 10^5 \text{ yr}$  and a rotational energy loss of  $\dot{E} = 4\pi^2 I P \dot{P}^{-3} \sim 3.0 \times 10^{34} \text{ erg s}^{-1}$  can be inferred. The average surface magnetic field is  $B_s \sim 2.2 \times 10^{12} \text{ G}$ , assuming a rotating dipolar model and a homogeneously magnetized sphere.

This pulsar has been detected with the *Hubble Space Telescope* by Mignani, Caraveo, & Bignami (1997), and by the X-ray satellites *Einstein* (Cheng & Helfand 1983), *EXOSAT* (Brinkmann & Ögelman 1987), *ROSAT* (Ögelman & Finley 1993), and *ASCA* (Greiveldinger et al. 1996). The combined *ROSAT* and *ASCA* data can be fitted by a two-blackbody

model with soft and hard components (Greiveldinger et al. 1996). The bolometric flux and temperature of the soft component are  $f_X^s = 7.8_{-2.0}^{+7.0} \times 10^{-12} \text{ erg cm}^{-2} \text{ s}^{-1}$  and  $T^s = 7.9_{-1.0}^{+0.6} \times 10^5 \text{ K}$ , respectively. The corresponding values for the hard component are  $f_X^h = 1.0_{-0.3}^{+0.7} \times 10^{-13} \text{ erg cm}^{-2} \text{ s}^{-1}$  and  $T^h = 3.7_{-1.2}^{+2.0} \times 10^6 \text{ K}$ . The flux ratio between both components is  $f_X^h/f_X^s = 0.013_{-0.008}^{+0.016}$ .

PSR B1055–52 is also one of the six  $\gamma$ -ray pulsars detected by the *Energetic Gamma Ray Experiment Telescope* (EGRET) on board the *Compton Gamma Ray Observatory* (CGRO), see Nolan et al. (1996). The first detection of pulsed high-energy  $\gamma$ -ray emission from this object was reported by Fierro et al. (1993). The total flux at energies  $E > 100 \text{ MeV}$  is  $\sim (2.7 \pm 0.5) \times 10^{-7} \text{ ph cm}^{-2} \text{ s}^{-1}$ , which corresponds to a total  $\gamma$ -ray luminosity  $L_\gamma \sim (9.6 \pm 1.6) \times 10^{33} \text{ erg s}^{-1}$  between 100 MeV and 5 GeV, if the distance to the source is  $\sim 1.5 \text{ kpc}$  and beaming into a solid angle of 1 sr is assumed. Such a luminosity implies

<sup>1</sup> Member of CONICET.

that PSR B1055-52 has by far the largest known efficiency for converting rotational energy in  $\gamma$ -rays:  $\eta = L_\gamma/\dot{E} \sim 31\%$ .

This efficiency, however, is a distance-dependent parameter, and it is important to remark that there has been some controversy about the actual distance to PSR B1055-52. Early estimates based on the dispersion measure yielded a distance of  $\sim 920$  pc (Manchester & Taylor 1981). More recent estimates with an improved Galactic electron density model suggest a distance of  $\sim 1500$  pc (Taylor, Manchester, & Lyne 1993). Using independent arguments, Ögelman & Finley (1993) proposed a distance of  $\sim 500$  pc. They considered that the softer blackbody temperature of the two-component spectral model fitting of the *ROSAT* data is produced by standard cooling of the neutron star and computed, using the bolometric flux, the distance required to keep the neutron star radius within a reasonable value.

A different distance estimate was obtained by Combi, Romero, & Azcárate (1997) by means of continuum radio observations of an extended non-thermal source that surrounds PSR B1055-52. They assumed that this emission is produced by relativistic pairs ejected by the pulsar, and calculated the maximum linear size of the synchrotron nebula which is compatible with the energy output of the pulsar and a standard set of parameters for the ISM, obtaining  $d \sim 700$  pc.

It is clear, then, that the question about the distance to PSR B1055-52 is far from being settled, and that there are some reasons to think that the dispersion measure distance might be overestimated. In this paper, we shall present a discussion of the possible mechanisms for the high-energy emission of PSR B1055-52 and their implications for the distance problem. Any consistent model of the production of high-energy photons in this pulsar must

be compatible with some observational parameters, like the luminosity ratio  $L_X/L_\gamma$ , which are distance-independent. If a given model fulfills this condition, then we can use it to estimate the distance to the pulsar by comparison of the predicted bolometric flux and the observed photon flux.

Throughout this paper we assume a radius  $R = 10^6$  cm for the neutron star and a standard moment of inertia  $I = 10^{45}$  g cm<sup>2</sup>. The angle  $\chi$  between the stellar magnetic moment and the spin axis is unknown. It has been argued (e.g., Lyne & Manchester 1988) that  $\chi$  can be obtained from the pulse width of the radio signal and the polarization properties. This approach yields for PSR B1055-52 a value of  $\sim 70^\circ$ . Model fittings of the spectral features of the  $\gamma$ -ray emission (e.g., Cheng & Ding 1994) suggest much lower values. Here, we shall adopt an intermediate value  $\chi = \pi/4$  for the numerical estimates and shall make explicit the dependence on  $\chi$  in the formulae. The basic pulsar parameters are listed in Table 1, while the main high-energy observational data are shown in Table 2.

## 2. ORIGIN OF THE HIGH-ENERGY EMISSION

It is widely accepted that the global current flow pattern through the magnetosphere of a rotating neutron star produces regions of charge depletion where  $\mathbf{E} \cdot \mathbf{B} \neq 0$  (the so-called "gaps"). In these regions the component of the electric field  $E_{||} = (\mathbf{E} \cdot \mathbf{B})/|\mathbf{B}|$  along the magnetic field lines can accelerate charged particles up to ultrarelativistic energies. Models for the high-energy emission of pulsars differ in the location of the acceleration region and the generation mechanism of the observable  $\gamma$ -ray photons.

In polar cap models particles are accelerated in gaps over the polar caps of the pulsar. These particles produce curvature  $\gamma$ -rays which are absorbed

TABLE 1

BASIC PULSAR PARAMETERS

Parameter	Symbol	Value
Period	$P$	0.19711 s
Period derivative	$\dot{P}$	$5.8 \times 10^{-15}$ s s <sup>-1</sup>
Angular velocity	$\Omega = 2\pi/P$	31.89 s <sup>-1</sup>
Dynamical age	$\tau$	$5.3 \times 10^5$ yr
Energy loss	$\dot{E}$	$3.0 \times 10^{34}$ erg s <sup>-1</sup>
Surface magnetic field <sup>a</sup>	$B_s$	$2.2 \times 10^{12}$ G
Stellar radius <sup>b</sup>	$R$	$10^6$ cm
Moment of inertia <sup>b</sup>	$I$	$10^{45}$ g cm <sup>2</sup>
Inclination angle <sup>b</sup>	$\chi$	$\pi/4$

<sup>a</sup> Assuming a rotating magnetic dipole model and  $\mu = B_s R^3/2$ .

<sup>b</sup> Assumed values.

TABLE 2  
HIGH-ENERGY OBSERVATIONAL PARAMETERS<sup>a</sup>

Parameter	Symbol	Value	Instrument	Ref. <sup>b</sup>
Soft blackbody X-ray component	$f_X^s$	$7.8^{+7.0}_{-2.0} \times 10^{-12} \text{ erg cm}^{-2} \text{ s}^{-1}$	<i>ROSAT + ASCA</i>	1, 2
Hard blackbody X-ray component	$f_X^h$	$1.0^{+0.7}_{-0.3} \times 10^{-13} \text{ erg cm}^{-2} \text{ s}^{-1}$	<i>ROSAT + ASCA</i>	1, 2
Hard to soft X-ray components ratio	$f_X^h/f_X^s$	$\sim 0.013$	<i>ROSAT + ASCA</i>	1, 2
$\gamma$ -ray flux ( $E > 100 \text{ MeV}$ )	$f_\gamma$	$(4.2 \pm 0.7) \times 10^{-10} \text{ erg cm}^{-2} \text{ s}^{-1}$	<i>EGRET</i>	3
Total X-ray to $\gamma$ -ray flux ratio	$f_X/f_\gamma$	$\sim 0.02$	<i>ROSAT + ASCA/EGRET</i>	1, 2, 3
Hard X-ray to $\gamma$ -ray flux ratio	$f_X^h/f_\gamma$	$\sim 2.3 \times 10^{-4}$	<i>ROSAT + ASCA/EGRET</i>	1, 2, 3

<sup>a</sup> All parameters are distance-independent.

<sup>b</sup> References: (1) Ögelman & Finley (1993); (2) Greiveldinger et al. (1996); (3) Fierro et al. (1993).

by one-photon pair production ( $\gamma + \mathbf{B} \rightarrow e^+ + e^-$ ) in the star magnetosphere, giving rise to a pair cascade. The observable  $\gamma$ -rays, which are beamed in the direction of the magnetic moment  $\mu$ , are then the result of curvature and synchrotron processes.

In outer gap models the particle acceleration occurs in charge-depleted regions of the outer magnetosphere near the null charge surface  $\Omega \cdot \mathbf{B} = 0$ . Pair production is achieved in these regions by two-photon pair production, where, for instance, one of the photons is an X-ray from the stellar surface and the other is a  $\gamma$ -ray (see Romani 1996 for details). The observable  $\gamma$ -ray emission is due to synchrotron and curvature radiation of secondary pairs. In Romani's version of the model the synchrotron component peaks at  $\sim 1$ –10 MeV while the  $E > 100 \text{ MeV}$  emission mainly corresponds to the curvature component.

In both types of models X-ray emission can be enhanced by return currents that heat the star polar caps. Non-thermal X-rays can be also expected in outer cap models. A broad review of high-energy radiation mechanisms in pulsars is given by Michel (1991). Here we shall concentrate in the application of these models to PSR B1055-52.

### 2.1. Polar Cap Model for PSR B1055-52

Polar cap models assume the formation of a relativistic pair plasma above the pulsar polar cap's ori-

nated in the magnetic field absorption of curvature  $\gamma$ -rays of electrons accelerated in the polar gap. Arons & Scharlemann (1979) and Arons (1981) have developed a quantitative treatment of the electrically driven flow including the poisoning of the electric field by the created electron-positron pairs, with the assumption of free electron emission from the stellar surface.

The Lorentz factor achieved by an accelerated primary electron in the gap potential  $\Phi$  is

$$\gamma_0 = \frac{e\Phi(H)}{mc^2}, \quad (1)$$

where  $\Phi$  is given by equation (41) of Arons (1981) and  $H$  is the height of the gap. Using the parameters for PSR B1055-52 (see Table 1) and assuming for simplicity a dipole magnetic field configuration we get that particles are injected above the pulsar polar cap with a Lorentz factor

$$\begin{aligned} \gamma_0 &\sim 2.3 \times 10^6 P^{-3/8} (\sin \chi)^{1/4}, \\ &\sim 3.9 \times 10^6. \end{aligned} \quad (2)$$

The total energy transported to the magnetosphere by these relativistic particles results

$$\begin{aligned} L_T &\sim 5 B_s R^3 P^{-19/8} \cos \chi (\sin \chi)^{1/4} \text{ erg s}^{-1}, \\ &\sim 2.8 \times 10^{32} \text{ erg s}^{-1}. \end{aligned} \quad (3)$$

Part of this energy will be transformed in  $\gamma$ -rays through curvature radiation. For primaries moving along dipole field lines, curvature emission produces a loss energy rate

$$\frac{d\gamma}{dt} = \frac{2}{3} \frac{e^2}{mc^3} \left( \frac{c}{R_c} \right)^2 \gamma^4, \quad (4)$$

where  $R_c \sim 10^{4.9} R^{1/2} P^{1/2}$  is the magnetic field line radius of curvature. Integrating equation (4) along a field line, we obtain the particle energy at a distance  $r$  from the center of the star for an initial energy  $\gamma_0$  (Ochelkov & Usov 1980; Harding 1981)

$$\gamma(r) = \gamma_0 \left[ 1 + \frac{9}{8} \frac{e^2 \Omega \gamma_0^3}{mc^3} \ln \left( \frac{r}{R} \right) \right]^{-1/3}. \quad (5)$$

Considering  $\gamma_f = \gamma(R_{lc})$ , where  $R_{lc} = c/\Omega \sim 9.4 \times 10^8$  cm is the radius of the light cylinder, we can estimate the  $\gamma$ -ray luminosity of PSR B1055-52 in the polar cap model as

$$L_\gamma \sim \frac{\gamma_0 - \gamma_f}{\gamma_0} L_T. \quad (6)$$

Since from equation (5)  $\gamma_f \approx 0.8\gamma_0$ , we get

$$L_\gamma \sim 6.8 \times 10^{31} \text{ erg s}^{-1}. \quad (7)$$

Bombardment of the polar cap by the return current of positrons trapped within the acceleration zone produces X-ray emission with a bolometric luminosity given by (Arons 1981)

$$L_X \sim 2 \times 10^{26} \mu_{30} P^{-27/8} (\sin \chi)^{5/4} \text{ erg s}^{-1}, \quad (8)$$

with an effective temperature

$$T_{\text{eff}} \sim 3 \times 10^5 \mu_{30}^{1/4} P^{-19/32} (\sin \chi)^{5/32} \text{ K}, \quad (9)$$

where  $\mu_{30}$  is the stellar magnetic moment in units of  $10^{30} \text{ G cm}^3$ . For PSR B1055-52 we obtain

$$L_X \sim 1.7 \times 10^{28} \text{ erg s}^{-1}, \quad (10)$$

$$T_{\text{eff}} \sim 6.4 \times 10^5 \text{ K}. \quad (11)$$

Thus, the polar cap model predicts a distance-independent ratio  $L_X/L_\gamma \sim 2.5 \times 10^{-4}$ , which is of the order of the ratio  $f_X^h/f_\gamma$  obtained for PSR B1055-52 from the combined *ROSAT* + *ASCA/EGRET* data (see Table 2). It is clear, however, that if the polar cap model is applied to explain the high-energy emission of this pulsar then a different model must be used to account for the soft X-ray emission. A

standard neutron star cooling model has been fitted to the *ROSAT* soft component data by Ögelmann & Finley (1993) with the result that the distance to the pulsar should be  $\sim 330$  pc if the neutron star radius is  $\sim 10^6$  cm as assumed here (for a radius of 15 km they estimate  $d \sim 500$  pc). These distances are inconsistent with the  $\sim 130$  pc required in order to accommodate the predicted  $\gamma$ -ray luminosity to the observed  $\gamma$ -ray flux (Table 2) and the assumed beaming (§ 1). The observed luminosity is  $L_\gamma = \Theta f_\gamma d^2$ , where  $\Theta$  is the beaming solid angle. We see, then, that the polar cap model requires relatively high beaming ( $\Theta \sim 0.19$  sr, which corresponds to an aperture angle for the beam of  $\sim 1.7^\circ$ ) to account for a distance of  $\sim 300$  pc. A very strong beaming factor  $\xi = \Theta/4\pi \sim 6 \times 10^{-4}$  must be assumed if the actual distance to the pulsar is the dispersion measure distance.

Outer gap models provide an alternative scenario for the high-energy emission of pulsars like PSR B1055-52, where the beaming requirements are not so compelling.

## 2.2. Outer Gap Model for PSR B1055-52

Cheng, Ho, & Ruderman (1986a,b) have developed a model for the radiation of rapidly spinning pulsars where the particle acceleration takes place in otherwise charge-depleted regions in the outer magnetosphere. In these regions, the electric field component along the magnetic field lines accelerates primary electrons/positrons in opposite directions to ultrarelativistic energies. The potential drop through the outer accelerator is

$$\Delta\Phi \sim 6 f^2 B_s P^{-2} \text{ V}, \quad (12)$$

where  $f$  is the fraction of the outer magnetosphere occupied by the gap. The number of particles accelerated by this potential per unit of time is

$$\frac{dN}{dt} \sim 2.5 \times 10^{18} f B_s P^{-2} \text{ s}^{-1}. \quad (13)$$

These particles are expected to generate primary  $\gamma$ -rays through inverse Compton scattering of tertiary lower energy photons. The  $\gamma$ -rays are energetic enough for producing secondary  $e^\pm$  pairs by interaction with the same tertiary photons. These pairs radiate secondary synchrotron/curvature  $\gamma$  and X-rays which in turn create new (tertiary) low energy pairs responsible for generating the tertiary synchrotron photons closing the loop. The secondary synchrotron  $\gamma$ -rays are the bulk of the detectable emission at *EGRET* energies. In a recent version of the model (Romani 1996) the soft photon background is provided by the thermal surface emission from the star. In such a picture the synchrotron emission peaks at the energy range of the *COMPTEL* detector of the

*CGRO*. The reader is referred to Romani's paper for further details.

In the canonical model the tertiary photons have a typical frequency (Cheng et al. 1986b)

$$\omega_s \sim \left(\frac{mc}{e\bar{B}}\right)^3 \left(\frac{mc^3\Omega}{e^2}\right)^2, \quad (14)$$

where  $\bar{B}$  is the averaged magnetic field in the gap. Ruderman & Cheng (1988) and Chen & Ruderman (1993) have argued that when the pulsar slows sufficiently down and consequently  $\omega_s$  diminishes in such a way that the pair-generation threshold cannot be achieved, it will no longer be possible to sustain the bootstrapped  $e^\pm$  production in the outer magnetosphere and then the  $\gamma$ -ray production is suppressed. As the pulsar slows down the outer magnetosphere becomes optically thin to  $\gamma$ -rays and the conversion efficiency  $\eta$  tends to unity. Finally, at a period

$$P_{dl} = 10^{-6} B_s^{5/12} \left(\frac{\Omega r_i}{c}\right)^{-5/4} \text{ s}, \quad (15)$$

the  $\gamma$ -ray emission ceases. In this equation  $r_i$  is the inner boundary of the outer gap, where the last closed field line intersects the  $\Omega \cdot \mathbf{B} = 0$  surface. The value of  $r_i$  is determined by both the angle  $\chi$  and the configuration of the magnetic field. For  $\chi \sim \pi/4$ , as we have assumed for PSR B1055-52,  $r_i \sim c/2\Omega$ . Using this value, we get that the death line for our pulsar occurs at  $P_{dl} \sim 0.330$  s. The  $\gamma$ -ray luminosity produced in the gap of a pulsar with a period close to  $P_{dl}$ , like PSR B1055-52, is (e.g., Usov 1994)

$$L_\gamma^s \sim \xi \frac{r_i[(P_{dl}/P)^{4/5} - 1]}{c/\Omega - r_i} I\Omega\dot{\Omega}, \quad (16)$$

where  $\xi \sim 1 - (P/P_{dl})^{4/5}$ . Clearly,  $L_\gamma^s = 0$  for  $P = P_{dl}$ . For  $P < P_{dl}$  the outer gap sustains pair production between  $r = r_i$  and  $r = r_i(P_{dl}/P)^{4/5}$  from  $\gamma + \gamma \rightarrow e^+ + e^-$  interactions, where the primary  $\gamma$ s are produced by inverse Compton losses of the accelerated particles. In the region between  $r = r_i(P_{dl}/P)^{4/5}$  and  $r = c/\Omega$  curvature  $\gamma$ -rays are the main source of energy loss for the particles. This emission contributes to the total  $\gamma$ -ray luminosity in such a way that the observable luminosity will be

$$L_\gamma^T \sim (1 - P/P_{dl})^{4/5} I\Omega\dot{\Omega}, \quad (17)$$

which for PSR B1055-52 yields  $L_\gamma^T \sim 8.5 \times 10^{33} \text{ erg s}^{-1}$ .

Near the death line the gap-averaged field is

$$\bar{B} \sim B_{lc} \left(\frac{P}{P_{dl}}\right)^{12/5}, \quad (18)$$

where  $B_{lc}$  is the field at the light cylinder given by

$$B_{lc} \sim B_s \left(\frac{\Omega R}{c}\right)^3. \quad (19)$$

Thus, for periods similar to that of PSR B1055-52 we have that the frequency of the tertiary photons (equation 14) has shifted from IR (as in Vela-like pulsars) to the optical band (Usov 1994)

$$\nu_s = \frac{\omega_s}{2\pi} \sim 1.3 \times 10^{15} \Omega^{1/5} \text{ Hz}, \quad (20)$$

In the case of PSR B1055-52 this frequency is  $\nu_s \sim 2.6 \times 10^{15} \text{ Hz}$ . These shifted tertiary photons would constitute the bulk of the optical emission recently detected by the *Hubble Space Telescope* in this pulsar (Mignani et al. 1997).

Copious X-ray emission can be produced in the outer gap model by relativistic particles which stream back to the neutron star along the field lines and strike the polar caps causing thermal emission. Particles in motion from the inner gap boundary to the stellar surface lose energy by curvature radiation. The Lorentz factor of a primary starting at  $r = r_i$  and moving along the last closed magnetic field line is (see equation 5)

$$\gamma(r) \sim \left[ \frac{9}{8} \frac{e^2 \Omega}{mc^3} \ln \left( \frac{r_i}{r} \right) \right]^{-1/3}, \quad (21)$$

for  $\gamma^3 \ll \gamma_0^3 = \gamma(r_i)^3$ . The curvature radiation illuminates the neutron star surface for particle distances shorter than

$$r_1 \sim R \left( \frac{4c}{\Omega R} \right)^{1/3}. \quad (22)$$

Then, the total energy that is transferred to the star per particle results

$$E(r_1) \sim \left[ \frac{9}{8} \frac{e^2 \Omega}{mc^3} \ln \left( \frac{r_i}{r_1} \right) \right]^{-1/3} mc^2. \quad (23)$$

Evaluating for PSR B1055-52 we obtain  $E(r_1) \sim 7.8 \text{ erg}$ . This energy will be re-emitted by the neutron star surface as X-rays. Using equation (13) we find that the total X-ray luminosity of PSR B1055-52 is  $L_X^T \sim 1.7 \times 10^{32} \text{ erg s}^{-1}$  for  $f \sim 0.15$ . In this case, the outer gap model predicts a distance-independent ratio  $L_X^T/L_\gamma^T \sim 0.02$ , in agreement with the observed  $f_X/f_\gamma$  ratio (see Table 2; also notice that due to the large observational errors  $f$  can be considerably larger).

Moreover, we can interpret the two-component X-ray spectrum as the result of the different penetration depth of ultrarelativistic primaries and their curvature  $\gamma$ -rays in the neutron star photosphere (Bogovalov & Kotov 1989; Harding, Ozerov, & Usov

1993). The  $\gamma$ -rays are absorbed in the magnetic field above the pulsar polar cap creating low energy electron/positron pairs. The energy of these secondary pairs and their synchrotron radiation is released and thermalized up to a few radiation lengths, forming a hot corona above the photosphere. Conversely, ultra-relativistic primaries penetrate deeply into the neutron star surface layers before thermalizing their energy. The result is a two-component X-ray spectrum where the ratio  $f_X^h/f_X^s$  considered as the ratio of curvature  $\gamma$ -rays to reverse primary particle energy flux is given by (Harding et al. 1993)

$$\frac{f_X^h}{f_X^s} \sim 10^{-14} \mu_{30}^{-1} R^2, \quad (24)$$

which for PSR B1055-52 yields  $f_X^h/f_X^s \sim 0.018$ , similar to the ratio obtained from the best two-blackbody fit of the combined *ROSAT* + *ASCA* data (Table 2).

We conclude that the outer gap model can provide a suitable description of the high-energy emission processes in PSR B1055-52 without high beaming requirements. In the next section we shall briefly discuss the implications for the distance estimate to this pulsar.

### 3. DISCUSSION

In Figure 1 we show the beaming solid angle required for the emission as a function of the distance for both types of models discussed in the previous section. The outer gap model can easily accommodate the observed  $\gamma$ -ray flux to large distances as required by the dispersion measure. The polar cap model, instead, demands high beaming to achieve the same results. However, if the actual distance is considerably shorter than 1.5 kpc, this latter model provides an attractive picture of the high-energy emission of PSR B1055-52 for a moderate beaming factor. Parsec-scale inhomogeneities in the cool ISM density towards the pulsar can lead to overestimate the distance when a global model for the Galactic electron density distribution is adopted as in Taylor et al. (1993).

The presence of a weak and extended continuum radio source of nonthermal nature around PSR B1055-52 (Combi et al. 1997) can be used to obtain a different distance estimate. This synchrotron source has been also detected by *ASCA* at hard X-rays (Shibata et al. 1997). The continuous pair production in both types of pulsar emission models results in oppositely directed  $e^+$  and  $e^-$  fluxes. Relativistic electrons stream away from the star magnetosphere and leave the light cylinder. These particles then diffuse with Alfvén velocity  $v_A = B/(4\pi\rho)^{1/2}$  in the ISM and emit radio waves by synchrotron mechanism in the Galactic magnetic field as described by Blandford et al. (1973). For an ISM with  $n \sim 1 \text{ cm}^{-3}$  and

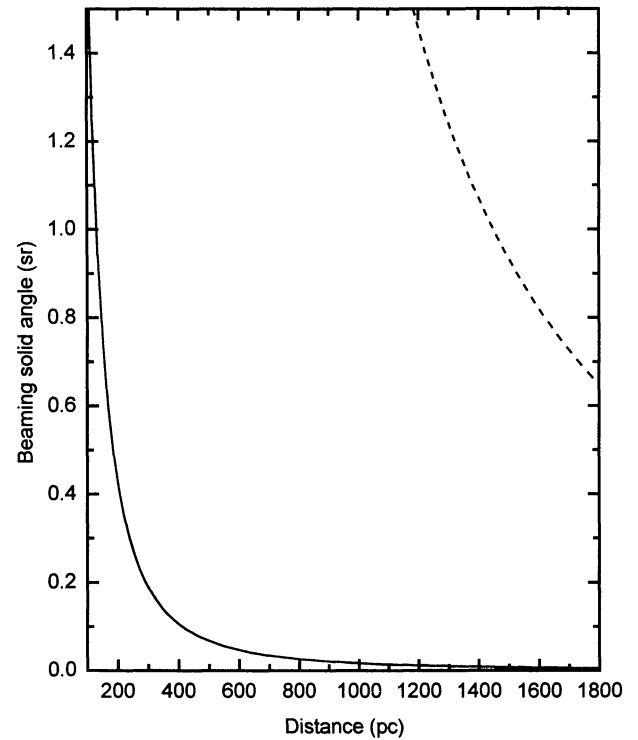


Fig. 1. Required beaming solid angle as a function of the distance for polar cap (solid line) and outer gap (dashed line) models of the high-energy emission of PSR B1055-52.

$B \sim 5 \times 10^{-6} \text{ G}$  results  $v_A \sim 11 \text{ km s}^{-1}$ , and then the particles could have reached distances of  $\sim 6 \text{ pc}$  from the star during the pulsar dynamical lifetime. The angular size of the diffuse radio source is  $\sim 1.5^\circ$ , implying a distance of  $\sim 460 \text{ pc}$ , similar to the independent estimate by Ögelman & Finley (1993). For such a distance the beaming factor of the polar cap model must be  $\xi \sim 6 \times 10^{-3}$ . The outer gap model requires  $\xi \sim 0.8$  for the same distance. This latter value corresponds to a beaming solid angle of  $\sim 10 \text{ sr}$ , which seems rather unrealistic (isotropy:  $4\pi$ ).

### 4. CONCLUSIONS

We have calculated the intrinsic  $\gamma$ -ray luminosities of PSR B1055-52 within polar cap and outer gap models which can account for distance-independent high-energy emission parameters obtained from recent satellite observations. If the actual distance to the pulsar is similar to the dispersion measure distance, then the most likely emission mechanism for this object seems to be that described by the outer gap picture. Beaming within  $1 \text{ sr}$  must be occurring in such a case. If, instead, the distance is considerably shorter ( $\sim 500 \text{ pc}$ ), polar cap emission with

moderate beaming should be the source of the observed high-energy radiation.

A key issue to decide the question is the non-thermal nebula that surrounds PSR B1055-52. New higher resolution observations of this nebula at different wavelengths would be crucial to clarify the distance problem and determine which is the dominant emission mechanism in this peculiar pulsar.

I am grateful to Z. Abraham and P. Benaglia for comments on the manuscript. This work has been supported by the Brazilian research agency FAPESP. Additional support from Argentinian PMT-PICT 0388 (ANPCT) is also acknowledged. An anonymous referee made a constructive criticism of an earlier version of this paper. I thank her/him very much.

#### REFERENCES

- Arons, J. 1981, *ApJ*, 248, 1099  
 Arons, J., & Scharlemann, E.T. 1979, *ApJ*, 231, 854  
 Blandford, R. D., Ostriker, J. P., Pacini, F., & Rees, M. J. 1973, *A&A*, 23, 145  
 Brinkmann, W., & Ögelman, H. 1987, *A&A*, 182, 71  
 Bogovalov, S. V., & Kotov, Yu. D. 1989, *Sov. Astr. Lett.* 15, 185  
 Chen, K., & Ruderman, M. A. 1993, *ApJ*, 402, 264  
 Cheng, A. F., & Helfand, D. J. 1983, *ApJ*, 271, 271  
 Cheng, K. S., Ho, C., & Ruderman, M. A. 1986a, *ApJ*, 300, 500  
 ———. 1986b, *ApJ*, 300, 522  
 Cheng, K. S., & Ding, W. K. Y. 1994, *ApJ*, 431, 724  
 Combi, J. A., Romero, G. E., & Azcárate, I. N. 1997, *Ap&SS*, 250, 1  
 Greiveldinger, C., et al. 1996, *ApJ*, 465, L35  
 Fierro, J. M., et al. 1993, *ApJ*, 413, L27  
 Harding, A. K. 1981, *ApJ*, 245, 267  
 Harding, A. K., Ozernoy, L. M., & Usov, V. V. 1993, *MNRAS*, 265, 921  
 Manchester, R. N., & Taylor, J. H. 1981, *AJ*, 86, 1954  
 Michel, F. C. 1991, *Theory of Neutron Star Magnetospheres*, (Chicago: Chicago Univ. Press.  
 Lyne, A. G., & Manchester, R. N. 1988, *MNRAS*, 234, 477  
 Mignani, R., Caraveo, P. A., & Bignami, G. F. 1997, *ApJ*, 474, L51  
 Nolan, P. L., et al. 1996, *A&AS*, 120, 61  
 Ochelkov, Yu. P., & Usov, V. V. 1980, *Ap&SS*, 69, 439  
 Ögelman, H., & Finley, J. P. 1993, *ApJ*, 413, L31  
 Romani, R.W. 1996, *ApJ*, 470, 469  
 Ruderman, M. A., & Cheng, K. S. 1988, *ApJ*, 335, 306  
 Shibata, S., et al. 1997, *ApJ*, 483, 843  
 Taylor, J. H., Manchester, R. N., & Lyne, A. G. 1993, *ApJS*, 88, 529  
 Vaughan, A. E., & Large, M. I. 1972, *MNRAS*, 156, 27  
 Usov, V.V. 1994, *ApJ*, 427, 394

Gustavo E. Romero: Instituto Astronômico e Geofísico, Universidade de São Paulo, Av. Miguel Stefano 4200, CEP 043010-904, São Paulo, SP, Brazil (gustavo@radio.iagusp.usp.br), and Instituto Argentino de Radioastronomía, CC 5, 1894 Villa Elisa, Bs. As., Argentina (romero@irma.iar.unlp.edu.ar).